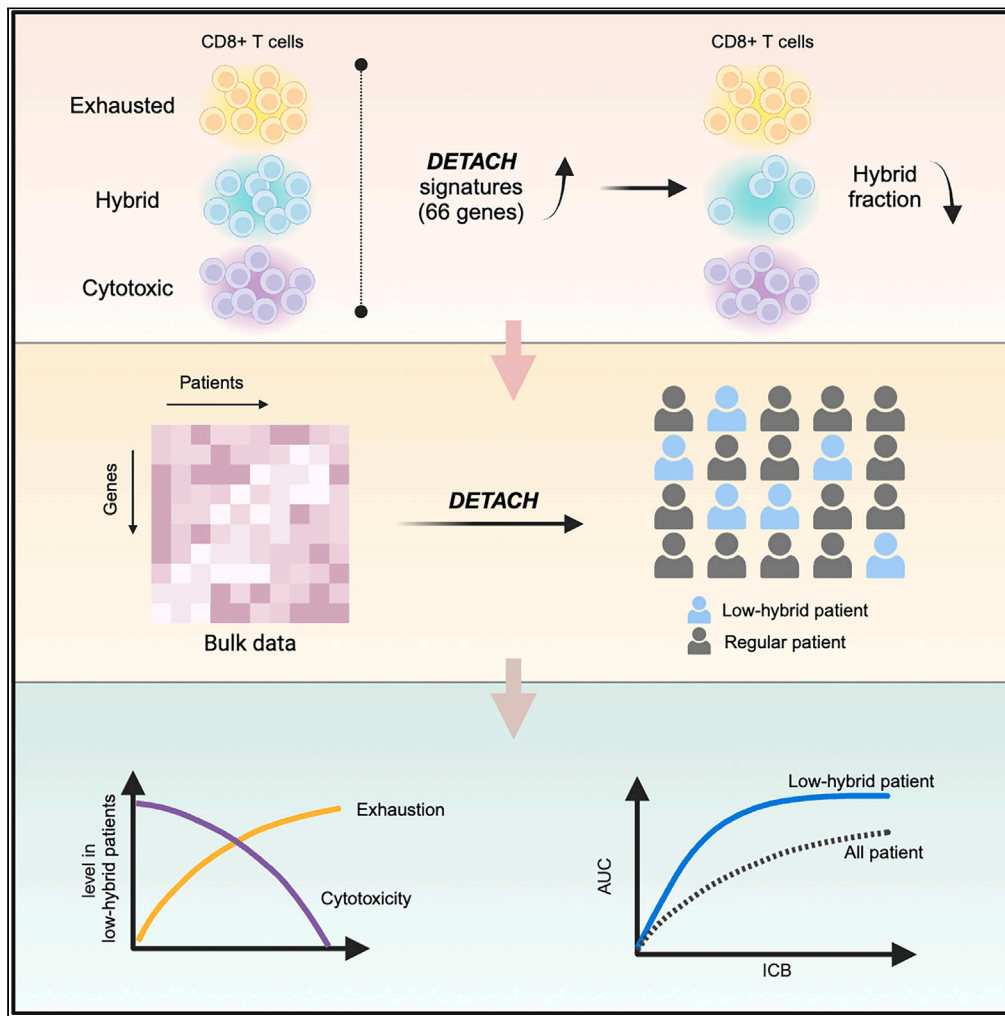**Article**

Decoupling the correlation between cytotoxic and exhausted T lymphocyte states enhances melanoma immunotherapy response prediction

Binbin Wang, Kun Wang, Di Wu, Sahil Sahni, Peng Jiang, Eytan Ruppin

eytan.ruppin@nih.gov

Highlights

DETACH successfully decouples CTL and ETL activities in bulk transcriptomic data

Decoupling CTL and ETL enhances ICI response prediction

DETACH is positively associated with tumor-reactive T cell infiltration and activation

Article

Decoupling the correlation between cytotoxic and exhausted T lymphocyte states enhances melanoma immunotherapy response prediction

Binbin Wang,[1,3] Kun Wang,[1,3] Di Wu,[2] Sahil Sahni,[1] Peng Jiang,[1] and Eytan Ruppin[1,4,*]

SUMMARY

Cytotoxic T lymphocyte (CTL) and terminal exhausted T lymphocyte (ETL) activities crucially influence immune checkpoint inhibitor (ICI) response. Despite this, the efficacy of ETL and CTL transcriptomic signatures for response prediction remains limited. Investigating this across the TCGA and publicly available single-cell cohorts, we find a strong positive correlation between ETL and CTL expression signatures in most cancers. We hence posited that their limited predictability arises due to their mutually canceling effects on ICI response. Thus, we developed DETACH, a computational method to identify a gene set whose expression pinpoints to a subset of melanoma patients where the CTL and ETL correlation is low. DETACH enhances CTL's prediction accuracy, outperforming existing signatures. DETACH signature genes activity also demonstrates a positive correlation with lymphocyte infiltration and the prevalence of reactive T cells in the tumor microenvironment (TME), advancing our understanding of the CTL cell state within the TME.

INTRODUCTION

Immune checkpoint inhibitors (ICIs) are one of the most important and effective therapeutic strategies rooted in cancer immunology. However, approximately half of melanoma patients remain unresponsive to ICI treatment. This underscores the pressing need to identify accurate biomarkers that can forecast which patients will benefit from ICIs. Moreover, there is a broader objective of anticipating novel and potentially more efficacious therapies. Cytotoxic T lymphocytes (CTL) play a pivotal role in shaping a patient's response to ICIs.[1,2] CTL activity, assessed through the expression of genes specific to CTLs,[3,4] has been frequently employed to predict ICIs response via bulk transcriptomics.[5–7] However, akin to other numerous transcriptomics-based biomarkers, its predictive efficacy has remained limited.[8–13] It is imperative to gain a comprehensive understanding of the cytotoxic states of cells to further optimize the utility of the CTL signature in predicting ICI responses.

CTL can encounter exhaustion due to the constant stimulation of cancer cells and immunosuppression within the tumor microenvironment (TME),[14–16] mediated via elevating inhibitory receptors (IRs) expression.[14] Such exhausted T cells are characterized by the loss of effector functions and elevated and sustained expression of inhibitory receptors.[14] The emergence of immune checkpoint blocking therapy as a strategy to treat cancer is based on the ability of monoclonal antibodies to block the interaction between specific IRs on exhausted T lymphocytes (ETL) and their corresponding ligands on cancer and other antigen-presenting cells.[17] Blocking such inhibitory interactions promotes the expansion and recovery of effector function in ETLs, leading to tumor regression in cancer patients. It's crucial to note, however, that the dysfunctional state of terminally exhausted T cells remains resistant to reprogramming by ICIs.[18,19] Recent studies have reported that majority of tumor neoantigen-specific CD8$^+$ T cells were in a state of exhaustion.[20,21] Furthermore, the cytotoxic and exhausted cell states, as defined by transcriptional signatures, are closely intertwined, potentially regulating common gene programs.[22–25] Collectively, these previous findings suggest that the conventional CTL gene signature alone may not be sufficient for assessing CTL activity in the TME following ICI treatment, thereby limiting its predictive power for ICI response.

In our analysis of both tumor TCGA bulk data and publicly available single-cell gene expression datasets we observed a robust positive correlation between CTL and ETL activities, estimated based on conventional gene signatures, across various cancer types. We hypothesized that this strong concordance between CTL and ETL activities in bulk expression may underlie the limited predictive capacity of CTL activity, potentially resulting in their activities mutually nullifying their antagonistic effects on ICI response. Decoupling these two activities could thus potentially enhance the predictive power of CTLs in ICI forecasting. Consequently, we have set out to develop a computational framework, DETACH (Decoupling ExhausTed And Cytotoxic lympHocytes), to identify a set of genes whose expression can pinpoint a subset of patients where the CTL and ETL correlation is diminished as much as possible. Within this framework, our initial

[1]Cancer Data Science Laboratory, Center for Cancer Research (CCR), National Cancer Institute (NCI), National Institutes of Health (NIH), Bethesda, MD USA
[2]Laboratory of Pathology, Center for Cancer Research (CCR), National Cancer Institute (NCI), National Institutes of Health (NIH), Bethesda, MD USA
[3]These authors contributed equally
[4]Lead contact
*Correspondence: eytan.ruppin@nih.gov

Figure 1. Characterization and decoupling of CTL and ETL activities

(A) The Pearson correlation between CTL and ETL activities, shown for many different cancer types in the TCGA cohort.

(B) A sample-wise scatterplot of CTL and ETL activities in TCGA skin cutaneous melanoma (SKCM) patients.

(C) The interaction multivariate linear regression used to identify the DETACH signature set of genes and is applied to all genes, one by one. Variables *E* and *G* represent the relation between T cell exhausted activity and expression of a given candidate gene, respectively. The coefficient of covariate ($E * G$) represents the conjunct interaction effect between *E* and *G* variables activity and CTL activity. The slopes between T cell cytotoxic and exhausted activity are shown by the arrow lines. Since the gene expressions used in this model are positive values, the change of the slope reflects the value of the coefficient $\beta 3$.

(D) The distribution of significance T values of all genes; those included in the DETACH signatures are colored in blue and a few top ones are specified; a negative T value of the covariate ($E * G$) for all tested genes indicates that the increased expression of this gene can mitigate the correlation between T cell cytotoxic and exhausted activity; if this effect is significant (STAR Methods) it is included in the DETACH signature set.

(E) DETACH signature score adjusted correlations between CTL and ETL activities versus those observed when using the random control signatures or the unadjusted (non-decoupled) correlations.

(F) CTL and ETL activities correlations in the high-DS-score patients' group (top 20 percent DS scores).

step involves identifying a group of genes whose overexpression significantly reduces the correlation between CTL and ETL, and we term this set as a "DETACH Signature" (DS). Utilizing the DS score, we can indeed pinpoint a subgroup of patients in whom CTL and ETL activities are effectively decoupled. Subsequently, this successful decoupling enhances the predictive capacity of CTL activity in forecasting ICI response among patients with high DS scores, yielding superior predictive accuracy when compared to existing state-of-the-art ICI predictive transcriptomic signatures.

RESULTS

Identifying a signature of genes whose upregulation identifies a subset of melanoma patients with reduced correlation between cytotoxic and exhausted T cell activities

To systemically characterize the association between CTL and ETL activities in bulk RNAseq data, we used established gene signatures of CTL[26] and ETL[19] activities. Given these signatures, we analyzed the bulk RNA-seq data via ssGSEA algorithm[27] to estimate CTL and

ETL activities in TCGA patients. By calculating the correlation between CTL and ETL activities across all samples in each cancer type, we found that the CTL and ETL activities were highly positively correlated in all cancer types (mean Pearson correlation: 0.65 ± 0.11) (Figures 1A and S1). The scatterplot of the two signatures activities across all melanoma samples is shown in Figure 1B. We hypothesized that this correlation may cancel out their opposing associations with ICI response and blunt the predictive power of CTL activity.

As melanoma has rich transcriptomic datasets of patients treated with ICIs, we decided to focus our study on this cancer type. In addition, melanoma has already quite a few published transcriptomics biomarker ICI signatures that we can compare with. We set out to study and validate the observed positive correlation between CTL and ETL activity, as seen in the bulk RNA-seq data in a cell-type manner, to ensure that this relationship was not influenced by variations in cell-type composition. First, we employed CODEFACS[28] to deconvolve the bulk TCGA SKCM RNA-seq data and estimate the gene expression that is specific to CD8^{+} T cells within each tumor sample, disentangling the effects of other cell types. Remarkably, we found that the strong positive correlation between the CTL and ETL activity is also evident in the expression of this specific cell-type (Figure S2A). This outcome substantially strengthens our initial observation, reinforcing the robustness of the correlation and its independence from cell type heterogeneity. Second, to further solidify the notion that this positive correlation is indeed inherent to CD8^{+} T cells, we collected data from three distinct melanoma single-cell cohorts, with each cohort comprising of a minimum of 20 patients.[29–31] Employing these datasets, our analysis conclusively demonstrates that the high correlation between CTL and ETL activity across patients in single-cell transcriptomics. (Figures S2B–S2D, STAR Methods). Furthermore, by examining the ETL and CTL activities of CD8^{+} T cells across three distinct cohorts, we identified a subset of CD8^{+} T cells with elevated levels of both ETL and CTL activities (Figures S3A–S3C). These findings underscore the interdependence of CTL and ETL activities as an inherent property of CD8^{+} T cells across diverse contexts, forming the basis of our research goal.

To decouple the CTL and ETL CD8^{+} T cell states, we developed DETACH, a computational method designed to identifying genes whose expression status mitigates the positive correlation between CTL and ETL activities. DETACH employs an interaction linear regression model in which the association between CTL and ETL activities can be represented by the coefficient denoting the slope of CTL and ETL activities (Figure 1C). Since the gene expression activities used in this model are positive values, the change in slope depends on the coefficients of the covariates.[32] A positive coefficient value indicates that higher expression of this gene increases the association of CTL and ETL activities, conversely, a negative value indicates that the higher expression of this gene reduces the association. We applied DETACH to TCGA melanoma datasets and identified a gene set of 66 genes (Figure 1D) (File S1), whose increased expression decouples CTL and ETL activities. We termed this gene set *the DETACH Signature (DS).* To assess DETACH's robustness, we applied it to down sampled subsets of the original training dataset. Notably, the original DETACH genes consistently appeared enriched at the top of the gene list identified within these sample subsets (Figure S4A). This robustness was further validated across independent melanoma cohorts[33–35] (Figure S4B). Subsequently, in each individual tumor sample, its *DS score* denotes the enrichment score of the DETACH signature, calculated using single samples Gene Set Enrichment Analysis algorithm (ssGSEA).[27] A high DS score indicates a weaker positive correlation between CTL and ETL activities. Specifically, when the DS score is high, high CTL activity corresponds to low ETL activity, and vice versa. Among the DETACH signature genes, some effector and memory T cell-associated genes[29,36,37] ranked in the top, such as *IFNG, TBX21,* and *GZMH.* The expression of these genes in the patients indicates that the CD8^{+} T cells in the TME were still functional and had not entered a dysfunctional state.

To verify the capability of the DETACH signature to decouple of CTL and ETL activities, we first calculated the DS scores for TCGA melanoma patients (labeled SKCM) and for five independent cohorts ICIs-treated melanoma patients (Gide,[33] Liu,[38] Riaz,[34] Cui,[39] and Van Allen[35]). We randomly selected the same number of genes as in the DETACH signature to serve as random control, comparison signatures (STAR Methods). We then employed a partial correlation analysis to compute the correlation between CTL and ETL activities after adjusting for the effect of the DETACH signature and that of a given control signature. Then, we compared both correlations to that of the original correlation (unadjusted) between the cytotoxic and exhausted signatures (Figure 1E). As expected, the correlation of CTL and ETL activities is indeed markedly decreased after adjusting for the DS score compared to that observed after adjusting to the control scores or to the original, unadjusted correlation (Figure 1E).

Moreover, to leverage the DETACH signature to enhance the predictive capability of CTL in ICB response, it is essential to establish an optimal threshold for the DS score, allowing for the selection of a high-DS-score patient group. This is driven by the premise that a higher DS score signifies lower correlation (between CTL and ETL) and greater prediction accuracy. The threshold for inclusion in the high-DS-score group was set according to two criteria: (1) to encompass as many patients as possible (at least 10%) in the high-DS-score group; (2) to minimize the correlation between CTL and ETL activity within the high-DS-score group. Initially, we established cohort-specific thresholds for both the TCGA and ICIs-treated melanoma cohorts (see Figure S5), adhering to the two specified criteria. It is crucial to highlight that this process maintains the integrity of avoiding data leakage, *as response label data were not involved in determining the threshold.* Leveraging the six cohort specific thresholds found in this procedure, we adopted the top 20% as a universal threshold to identify patients with high DS scores. Subsequently, we isolated a subset of patients representing the top 20% with high DS scores. In both the training dataset (TCGA melanoma) and the testing datasets (melanoma treated with ICIs), the high DS score groups exhibit a significant lower correlation between CTL and ETL activities, as anticipated (Figure 1F). It is worth noting that the correlation between ETL and CTL was not diminished significantly in Liu et al. and Cui et al. datasets compared to other datasets. This may be attributed to the use of FFPE samples for RNAseq in Liu et al. and Cui et al., while other datasets utilized frozen specimens for extracting the gene expression signature, similar to the TCGA samples, where the DETACH signature was derived
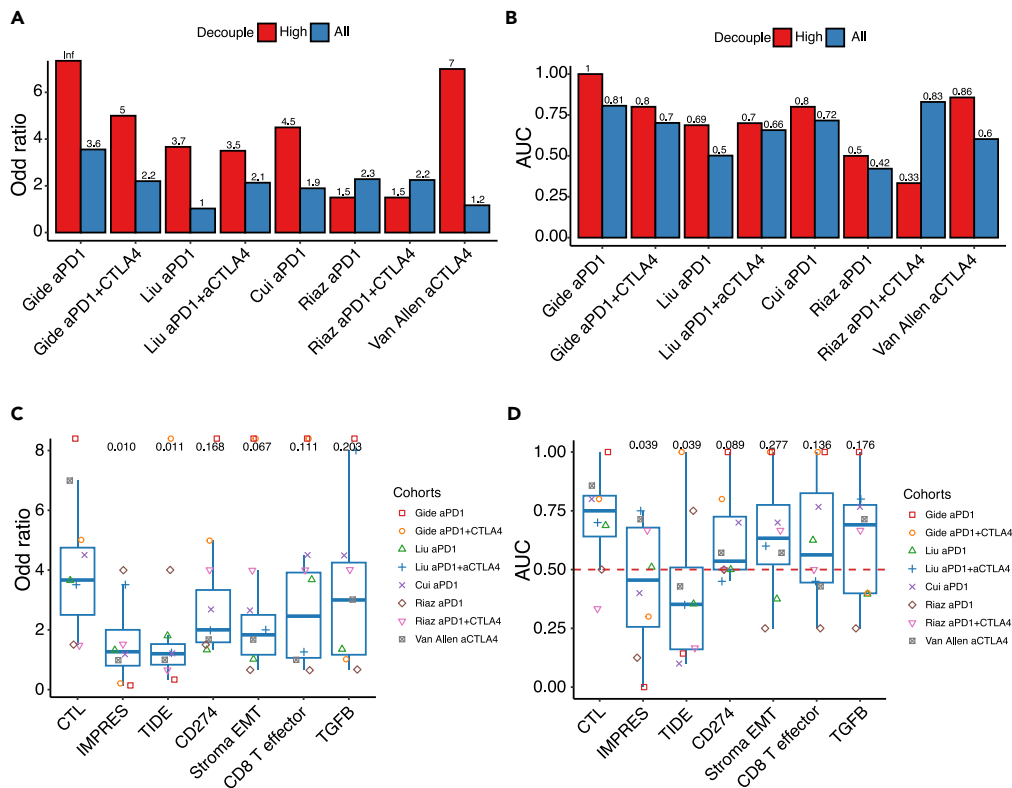
Figure 2. CTL activity is strongly predictive of ICI response in high-DS-score patients

Bar plots showing the accuracy of ICI response prediction for cytotoxic activity in different melanoma cohorts. This is shown in terms of both odds ratio (A) and area under the ROC curve (AUC, B) in the high DS groups compared to the groups that include all patients. The Riaz Pre CTLA4 treatment group of patients with high DS scores was excluded from this analysis as it does not include any non-responders. The odds ratio (C) and AUC (D) quantifying ICI prediction performance of CTL to the previously established transcriptomics-based signatures in the high-DS-score patients. One-sided p values were displayed at the top of each box and were calculated using a paired Wilcoxon rank test to compare the control (CTL) group with other signatures. In all panels the four ICI-treated melanoma cohorts studied are sub-divided into seven cohorts according to the treatments the patients have received.

from. These results affirm the capacity of the TCGA-inferred DETACH signature to reduce the correlation between CTLs and ETL activities.

CTL activity is highly predictive of ICI response in high DS-score melanoma patients

We turned to assess the performance of CTL activity in predicting ICIs response in the high-DS-score patients (top 20% patient group). We measured the prediction performance of CTL activity in five independent ICI cohorts using two complementary standard measures, the area under the receiver operating curve (AUC) and the Odds ratio of responders to non-responders (OR). The AUC is a standard measure in machine learning for evaluating the overall predictive performance of a classifier across all possible decision thresholds. The OR denotes the odds to respond when the treatment is recommended divided by the odds when the treatment is not recommended. It quantifies the performance at a chosen decision threshold and is hence a more clinically oriented measure (STAR Methods). In 7 of the 8 treatment groups we studied, CTL activity achieved better performance in the prediction of ICIs response in the high-DS-score (Figures 2A and 2B). Subsequently, we evaluated the predictive efficacy of CTL activity on this patients group in comparison to various other contemporary transcriptomics-based ICI response prediction methods and biomarkers, TIDE,[7] IMPRES,[40] CD274 (PDL1),[13] stroma EMT,[41] CD8 T cell effector,[42] and TGFB[43] (STAR Methods) in the high DS score patient group. We find that CTL activity exhibits a substantially superior performance compared to other methods and biomarkers. However, it is important to acknowledge that not all of the observed differences reached statistical significance, likely due to the limited sample size (Figures 2C and 2D). Moreover, we have observed that CTL activity exhibits superior performance in predicting ICI response among patients with high DS scores, as determined using a cohort-specific threshold (Figure S6, STAR Methods). These findings propose a potential two-stage approach for stratifying melanoma patients for ICI treatment based on bulk tumor expression: (1) Initially, ascertain whether a patient possesses a high DS score, which can be achieved through either a global threshold (top 20th percentile) or a cohort-specific threshold. (2) If the patient meets the criteria for a high DS score, proceed to assess their response to ICI treatment based on the CTL score computed from their tumor expression.
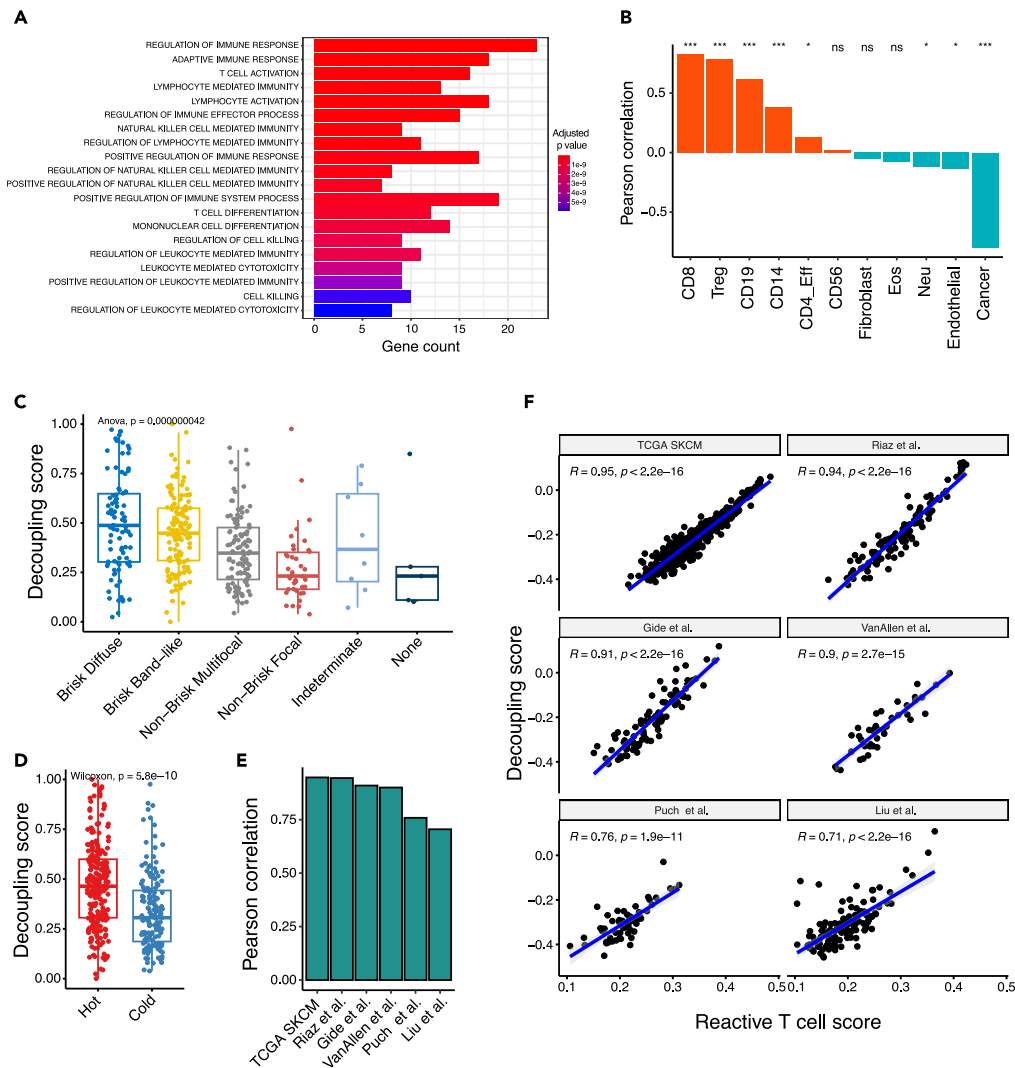
Figure 3. DETACH signature activity is associated with T cell activation, immune cell infiltration, and antigen-specific reactive T cell activity

(A) Pathway enrichment analysis of DETACH signature genes; the x axis represents the number of DETACH signature genes in each enriched pathway, the colors represent the corresponding enrichment hypergeometric statistical significance, as indicated in the color schema on the right side (STAR Methods).

(B) The correlation between the DS score and cell abundances across TCGA SKCM; the stars at the top denote significance values (STAR Methods). *$p < 0.05$, **$p < 0.01$, ***$p < 0.001$, ns p>=0.05.

(C) The distribution of DS scores among patients with different pathology-determined lymphocyte infiltration status.

(D) The distribution of DS scores in hot versus cold tumors.

(E) Bar plot illustrating the correlation between the reactive T cell score and DS score across six distinct melanoma cohorts.

(F) Scatterplots depicting the relationship between DS scores and tumor antigen-specific reactive T cell activity scores across six distinct melanoma patient cohorts. Each data point represents an individual patient.

The DETACH signature activity is strongly positively associated with T cell activation and immune cell infiltration in melanoma

To further characterize the biological pathways contributing to the DETACH signature, we identified the pathways enriched in these genes (STAR Methods). Those point to T cell activation/differentiation and lymphocyte activation and differentiation (Figure 3A). Furthermore, the DS scores are positively correlated with computationally estimated T CD8, T CD4, macrophage, and B cell abundances (STAR Methods, Figure 3B). Notably, they are anti-correlated with abundance of tumor cells (a correlate of tumor purity).

We next set out to study to what extent is the DETACH signature genes activity associated with estimates of T cell abundance and infiltration done by pathologists reviewing tumor H&E slides. To test that, we retrieved lymphocyte status annotations of TCGA melanoma patients from a study that assessed lymphocyte status based on pathological slides data.[44] In this study, patients were assigned to one of five patterns based on tumor-infiltrating lymphocyte status: Brisk diffuse, Brisk band-like, Non-brisk multi-focal, Non-brisk focal, and None[44]

(STAR Methods). Due to its limited sample size, we filtered the "None" group from further analysis. "Brisk" denotes a "hot" tumor displaying a moderate to strong immune response, characterized by the presence of diffusely infiltrative scattered TILs covering at least 30% of the tumor's area or forming band-like boundaries along the tumor's periphery. Conversely, "Non-brisk" indicates a "cold" tumor signifying a weak immune response, with sparsely scattered TILs confined to a small region within the tumor. By comparing the distribution of DS scores between samples in the different patterns, we find that the DS scores are positively associated with tumor-infiltrating lymphocytes abundance and infiltration in melanoma (Figure 3C). We then classified patients dichotomously into "Hot" (Brisk diffuse, Brisk Band-like) and "Cold" tumors (Non-brisk multi-focal, Non-brisk focus, None). Again, we find that "Hot" tumors have significantly higher DS scores than "Cold" tumors (Figure 3D). Taking together, these strong associations indicate that in tumors highly infiltrated by T cells, the CTL and ETL activities are relatively lowly correlated, suggesting that the activated CD8$^+$ T cells are indeed pre-exhausted.

Previous studies have shown that tumor-infiltrating CD8$^+$ T cells consist of virus-specific bystander T cells and tumor antigen-specific reactive T cells.[45,46] A recent study characterized antigen-specific reactive T cells by combining single-cell sequencing and TCR sequencing technologies.[47] To study the association between DS scores and tumor antigen-specific reactive T cell activity, we estimated the reactive T cell activity in each patient's tumor in the melanoma cohorts we study, based on the reactive T cell activity signature.[47] As the tumor bulk expression is a mixture of all cell types in the tumor microenvironment, we used the deconvoluted gene expression profiles of CD8$^+$ T cells[28] to estimate the reactive T cell activity in melanoma patients in the different cohorts we have studied. Notably, we find that the DS scores are highly positively correlated with the estimated reactive antigen-specific T cell activities (Figures 3E and 3F). Of interest, among the transcriptomic-based ICB prediction signatures, our DS score, CTL and effector T cell signatures exhibit stronger positive correlation with reactive antigen-specific T cell activities compared to other methods (Figure S7). These results suggest that the DS score is not only associated with the overall abundance of TILs but also of with the abundance of tumor antigen-specific reactive T cells. It further supports that the notion that in the subset of tumors where the CTL and ETL activities are not correlated, the tumor environment is indeed enriched with cytotoxic non-exhausted and reactive T cells. Additionally, these results underscore the importance of reactive T cell activity in CD8 T cell-based predictors (CTL, effector T cell) for predicting ICB response.

DISCUSSION

Motivated by the correlations observed between cytotoxic lymphocyte (CTL) and exhausted T cell lymphocyte (ETL) activities inferred from both bulk and single-cell RNAseq data across various cancer types, our primary aim was to formulate a computational framework capable of discerning their distinct contributions. In this study, we introduced DETACH, a computational approach to effectively segregate CTL and ETL activities in melanoma. Importantly, DETACH rescues the prognostic value of CTL activity for predicting the response of melanoma patients to immune checkpoint inhibitors within a subgroup of high-scoring patients, surpassing the predictive capacity of other contemporary transcriptomics-based models. The genes comprising the DETACH signature are enriched in pathways associated with immune responses, particularly T cell activation and differentiation. The DS score exhibits a positive correlation with lymphocyte infiltration and a negative correlation with estimates of tumor purity. These findings imply that the predictive power of CTL in anticipating immune checkpoint blockade response is contingent on the extent of T cell infiltration, as indicated by the magnitude of the DETACH signature.

The results presented herein introduce a conceptually innovative approach for stratifying patients for immune checkpoint inhibitor (ICI) therapy by leveraging the sequential application of two transcriptomic-based biomarkers. This approach does come with an inherent trade-off, as it achieves heightened predictive accuracy within a restricted subset of high-scoring patients, rather than across the entire population. Nevertheless, this tradeoff is justified as it enables to attain a higher degree of accurate patients stratification, albeit on a subset of the patients. Furthermore, it is imperative to acknowledge that our current investigation is confined to melanoma, and exploring the potential applicability of the presented approach in predicting ICI response across various other cancer types warrants further investigation in future prospective studies. While our functional analysis has provided valuable insights into the identified DETACH signature, our comprehension of how these signatures mediate the efficacy of CTL remains somewhat limited. One hand, we hypothesize that the DETACH signature genes are additional signature genes for CTLs, higher DS levels indicate more likely CTLs. On the other hand, due to the observed association with TILs and abundance of reactive T cells, the DS score could imply that beyond the activity level, the abundance of CTLs also plays a major role in mediating ICI response.

This study demonstrates the utility of our dual-pronged approach in predicting patient responses, specifically focusing on those whose DS scores exceed a predetermined threshold. Our emphasis lies in leveraging bulk transcriptomics, a data type abundant with valuable clinical information. While previous studies have widely employed CTL signatures for ICI response prediction using bulk transcriptomics, their predictive accuracy has been limited. Our study offers a potential explanation and a solution addressing this limitation. As the correlation between CTL and ETL remains intact in single-cell data, our approach may hold promise in providing further insights into this type of data in future research endeavors.

In summary, we have introduced a computational method, facilitating a two-step approach for predicting ICI response specifically for patients in the higher-score group, utilizing CTL signatures. This method significantly bolsters the effectiveness of CTLs in ICI prediction and enhances our understanding of the mediating role of CTLs within the TME.

Limitations of the study

Our study primarily focuses on melanoma, limiting the generalizability of our findings to other cancer types. Further investigation across diverse cancer cohorts is necessary to ascertain the broader applicability of the DETACH framework. It's important to acknowledge that

only a subset of patients may benefit from the DETACH framework due to its reliance on identifying high-scoring patients. This selective applicability may limit its broader utility across all melanoma patients.

STAR★METHODS

Detailed methods are provided in the online version of this paper and include the following:

- KEY RESOURCES TABLE
- RESOURCE AVAILABILITY
  - Lead contact
  - Materials availability
  - Data and code availability
- METHOD DETAILS
  - Transcriptomic data and gene signatures
  - Prediction of ICIs response, patient cohort and clinical end points
  - DETACH
  - Determination of thresholds for patients with high DS score
  - Robustness evaluation of DETACH signature
  - TCGA Tumor Infiltrated Lymphocyte (TIL) patterns
  - Gene function enrichment analysis
- QUANTIFICATION AND STATISTICAL ANALYSIS

SUPPLEMENTAL INFORMATION

Supplemental information can be found online at https://doi.org/10.1016/j.isci.2024.109926.

AUTHOR CONTRIBUTIONS

B.W., K.W., and E.R. designed the study. B.W. and K.W. conducted computational analyses and developed the DETACH algorithm. K.W., B.W., and S.S. collected bulk ICB RNA-seq data. D.W. generated the graphic abstract. B.W. drafted the original manuscript, while K.W., P.J., and E.R. revised it. All authors reviewed and approved the final manuscript.

DECLARATION OF INTERESTS

E.R. is a co-founder of Medaware Ltd. (https://www.medaware.com/), Metabomed (https://www.metabomed.com/), and Pangea Biomed (https://pangeamedicine.com/). He has divested and serves as an unpaid scientific consultant to the latter company.

DECLARATION OF GENERATIVE AI AND AI-ASSISTED TECHNOLOGIES IN THE WRITING PROCESS

During the preparation of this work, the authors used ChatGTP 3.5 in order to improve the writing for some sentences in this paper. After using this tool, the authors reviewed and edited the content as needed and take full responsibility for the content of the published article.

REFERENCES

1. Farhood, B., Najafi, M., and Mortezaee, K. (2019). CD8⁺ cytotoxic T lymphocytes in cancer immunotherapy: A review. J. Cell. Physiol. 234, 8509–8521. https://doi.org/10.1002/jcp.27782.

2. Au, L., Hatipoglu, E., Robert de Massy, M., Litchfield, K., Beattie, G., Rowan, A., Schnidrig, D., Thompson, R., Byrne, F., Horswell, S., et al. (2021). Determinants of anti-PD-1 response and resistance in clear cell renal cell carcinoma. Cancer Cell 39,

1497–1518.e11. https://doi.org/10.1016/j.ccell.2021.10.001.

3. Rooney, M.S., Shukla, S.A., Wu, C.J., Getz, G., and Hacohen, N. (2015). Molecular and Genetic Properties of Tumors Associated with Local Immune Cytolytic Activity. Cell 160, 48–61. https://doi.org/10.1016/j.cell.2014.12.033.

4. Jiang, P., Gu, S., Pan, D., Fu, J., Sahu, A., Hu, X., Li, Z., Traugh, N., Bu, X., Li, B., et al. (2018).

Signatures of T cell dysfunction and exclusion predict cancer immunotherapy response. Nat. Med. 24, 1550–1558. https://doi.org/10.1038/s41591-018-0136-1.

5. Lozano, A.X., Chaudhuri, A.A., Nene, A., Bacchiocchi, A., Earland, N., Vesely, M.D., Usmani, A., Turner, B.E., Steen, C.B., Luca, B.A., et al. (2022). T cell characteristics associated with toxicity to immune checkpoint blockade in patients with

melanoma. Nat. Med. *28*, 353–362. https://doi.org/10.1038/s41591-021-01623-z.

6. Hsu, C.-L., Ou, D.-L., Bai, L.-Y., Chen, C.-W., Lin, L., Huang, S.-F., Cheng, A.-L., Jeng, Y.-M., and Hsu, C. (2021). Exploring Markers of Exhausted CD8 T Cells to Predict Response to Immune Checkpoint Inhibitor Therapy for Hepatocellular Carcinoma. Liver Cancer *10*, 346–359. https://doi.org/10.1159/000515305.

7. Pender, A., Titmuss, E., Pleasance, E.D., Fan, K.Y., Pearson, H., Brown, S.D., Grisdale, C.J., Topham, J.T., Shen, Y., Bonakdar, M., et al. (2021). Genome and Transcriptome Biomarkers of Response to Immune Checkpoint Inhibitors in Advanced Solid Tumors. Clin. Cancer Res. *27*, 202–212. https://doi.org/10.1158/1078-0432.CCR-20-1163.

8. Litchfield, K., Reading, J.L., Puttick, C., Thakkar, K., Abbosh, C., Bentham, R., Watkins, T.B.K., Rosenthal, R., Biswas, D., Rowan, A., et al. (2021). Meta-analysis of tumor- and T cell-intrinsic mechanisms of sensitization to checkpoint inhibition. Cell *184*, 596–614.e14. https://doi.org/10.1016/j.cell.2021.01.002.

9. Narayanan, S., Kawaguchi, T., Yan, L., Peng, X., Qi, Q., and Takabe, K. (2018). Cytolytic Activity Score to Assess Anticancer Immunity in Colorectal Cancer. Ann. Surg Oncol. *25*, 2323–2331. https://doi.org/10.1245/s10434-018-6506-6.

10. Tumeh, P.C., Harview, C.L., Yearley, J.H., Shintaku, I.P., Taylor, E.J.M., Robert, L., Chmielowski, B., Spasic, M., Henry, G., Ciobanu, V., et al. (2014). PD-1 blockade induces responses by inhibiting adaptive immune resistance. Nature *515*, 568–571. https://doi.org/10.1038/nature13954.

11. Loi, S., Adams, S., Schmid, P., Cortés, J., Cescon, D.W., Winer, E.P., Toppmeyer, D.L., Rugo, H.S., De Laurentiis, M., Nanda, R., et al. (2017). LBA13 - Relationship between tumor infiltrating lymphocyte (TIL) levels and response to pembrolizumab (pembro) in metastatic triple-negative breast cancer (mTNBC): Results from KEYNOTE-086. Ann. Oncol. *28*, v608. https://doi.org/10.1093/annonc/mdx440.005.

12. Hamid, O., Schmidt, H., Nissan, A., Ridolfi, L., Aamdal, S., Hansson, J., Guida, M., Hyams, D.M., Gómez, H., Bastholt, L., et al. (2011). A prospective phase II trial exploring the association between tumor microenvironment biomarkers and clinical activity of ipilimumab in advanced melanoma. J. Transl. Med. *9*, 204. https://doi.org/10.1186/1479-5876-9-204.

13. Gibney, G.T., Weiner, L.M., and Atkins, M.B. (2016). Predictive biomarkers for checkpoint inhibitor-based immunotherapy. Lancet Oncol. *17*, e542–e551. https://doi.org/10.1016/S1470-2045(16)30406-5.

14. McLane, L.M., Abdel-Hakeem, M.S., and Wherry, E.J. (2019). CD8 T Cell Exhaustion During Chronic Viral Infection and Cancer. Annu. Rev. Immunol. *37*, 457–495. https://doi.org/10.1146/annurev-immunol-041015-055318.

15. Wherry, E.J. (2011). T cell exhaustion. Nat. Immunol. *12*, 492–499. https://doi.org/10.1038/ni.2035.

16. Chu, Y., Dai, E., Li, Y., Han, G., Pei, G., Ingram, D.R., Thakkar, K., Qin, J.-J., Dang, M., Le, X., et al. (2023). Pan-cancer T cell atlas links a cellular stress response state to immunotherapy resistance. Nat. Med. *29*,

1550–1562. https://doi.org/10.1038/s41591-023-02371-y.

17. Sharma, P., and Allison, J.P. (2015). Immune Checkpoint Targeting in Cancer Therapy: Toward Combination Strategies with Curative Potential. Cell *161*, 205–214. https://doi.org/10.1016/j.cell.2015.03.030.

18. Liu, B., Hu, X., Feng, K., Gao, R., Xue, Z., Zhang, S., Zhang, Y., Corse, E., Hu, Y., Han, W., and Zhang, Z. (2022). Temporal single-cell tracing reveals clonal revival and expansion of precursor exhausted T cells during anti-PD-1 therapy in lung cancer. Nat. Cancer *3*, 108–121. https://doi.org/10.1038/s43018-021-00292-8.

19. Philip, M., Fairchild, L., Sun, L., Horste, E.L., Camara, S., Shakiba, M., Scott, A.C., Viale, A., Lauer, P., Merghoub, T., et al. (2017). Chromatin states define tumour-specific T cell dysfunction and reprogramming. Nature *545*, 452–456. https://doi.org/10.1038/nature22367.

20. Oliveira, G., Stromhaug, K., Klaeger, S., Kula, T., Frederick, D.T., Le, P.M., Forman, J., Huang, T., Li, S., Zhang, W., et al. (2021). Phenotype, specificity and avidity of antitumour CD8+ T cells in melanoma. Nature *596*, 119–125. https://doi.org/10.1038/s41586-021-03704-y.

21. Caushi, J.X., Zhang, J., Ji, Z., Vaghasia, A., Zhang, B., Hsiue, E.H.-C., Mog, B.J., Hou, W., Justesen, S., Blosser, R., et al. (2021). Transcriptional programs of neoantigen-specific TIL in anti-PD-1-treated lung cancers. Nature *596*, 126–132. https://doi.org/10.1038/s41586-021-03752-4.

22. Tirosh, I., Izar, B., Prakadan, S.M., Wadsworth, M.H., Treacy, D., Trombetta, J.J., Rotem, A., Rodman, C., Lian, C., Murphy, G., et al. (2016). Dissecting the multicellular ecosystem of metastatic melanoma by single-cell RNA-seq. Science *352*, 189–196. https://doi.org/10.1126/science.aad0501.

23. Doering, T.A., Crawford, A., Angelosanto, J.M., Paley, M.A., Ziegler, C.G., and Wherry, E.J. (2012). Network Analysis Reveals Centrally Connected Genes and Pathways Involved in CD8+ T Cell Exhaustion versus Memory. Immunity *37*, 1130–1144. https://doi.org/10.1016/j.immuni.2012.08.021.

24. Fuertes Marraco, S.A., Neubert, N.J., Verdeil, G., and Speiser, D.E. (2015). Inhibitory Receptors Beyond T Cell Exhaustion. Front. Immunol. *6*, 310.

25. Singer, M., Wang, C., Cong, L., Marjanovic, N.D., Kowalczyk, M.S., Zhang, H., Nyman, J., Sakuishi, K., Kurtulus, S., Gennert, D., et al. (2016). A Distinct Gene Module for Dysfunction Uncoupled from Activation in Tumor-Infiltrating T Cells. Cell *166*, 1500–1511.e9. https://doi.org/10.1016/j.cell.2016.08.052.

26. Kim, N., Kim, H.K., Lee, K., Hong, Y., Cho, J.H., Choi, J.W., Lee, J.-I., Suh, Y.-L., Ku, B.M., Eum, H.H., et al. (2020). Single-cell RNA sequencing demonstrates the molecular and cellular reprogramming of metastatic lung adenocarcinoma. Nat. Commun. *11*, 2285. https://doi.org/10.1038/s41467-020-16164-1.

27. Subramanian, A., Tamayo, P., Mootha, V.K., Mukherjee, S., Ebert, B.L., Gillette, M.A., Paulovich, A., Pomeroy, S.L., Golub, T.R., Lander, E.S., and Mesirov, J.P. (2005). Gene set enrichment analysis: A knowledge-based approach for interpreting genome-wide expression profiles. Proc. Natl. Acad. Sci. USA *102*, 15545–15550. https://doi.org/10.1073/pnas.0506580102.

28. Wang, K., Patkar, S., Lee, J.S., Gertz, E.M., Robinson, W., Schischlik, F., Crawford, D.R., Schaffer, A.A., and Ruppin, E. (2022). Deconvolving clinically relevant cellular immune crosstalk from bulk gene expression using CODEFACS and LIRICS stratifies melanoma patients to anti-PD-1 therapy. Cancer Discov. *12*, 1088–1105. candisc.0887.2021. https://doi.org/10.1158/2159-8290.CD-21-0887.

29. Li, H., van der Leun, A.M., Yofe, I., Lubling, Y., Gelbard-Solodkin, D., van Akkooi, A.C.J., van den Braber, M., Rozeman, E.A., Haanen, J.B.A.G., Blank, C.U., et al. (2019). Dysfunctional CD8 T Cells Form a Proliferative, Dynamically Regulated Compartment within Human Melanoma. Cell *176*, 775–789.e18. https://doi.org/10.1016/j.cell.2018.11.043.

30. Jerby-Arnon, L., Shah, P., Cuoco, M.S., Rodman, C., Su, M.-J., Melms, J.C., Leeson, R., Kanodia, A., Mei, S., Lin, J.-R., et al. (2018). A Cancer Cell Program Promotes T Cell Exclusion and Resistance to Checkpoint Blockade. Cell *175*, 984–997.e24. https://doi.org/10.1016/j.cell.2018.09.006.

31. Sade-Feldman, M., Yizhak, K., Bjorgaard, S.L., Ray, J.P., de Boer, C.G., Jenkins, R.W., Lieb, D.J., Chen, J.H., Frederick, D.T., Barzily-Rokni, M., et al. (2018). Defining T Cell States Associated with Response to Checkpoint Immunotherapy in Melanoma. Cell *175*, 998–1013.e20. https://doi.org/10.1016/j.cell.2018.10.038.

32. Jiang, P., Lee, W., Li, X., Johnson, C., Liu, J.S., Brown, M., Aster, J.C., and Liu, X.S. (2018). Genome-Scale Signatures of Gene Interaction from Compound Screens Predict Clinical Efficacy of Targeted Cancer Therapies. Cell Syst. *6*, 343–354.e5. https://doi.org/10.1016/j.cels.2018.01.009.

33. Gide, T.N., Quek, C., Menzies, A.M., Tasker, A.T., Shang, P., Holst, J., Madore, J., Lim, S.Y., Velickovic, R., Wongchenko, M., et al. (2019). Distinct Immune Cell Populations Define Response to Anti-PD-1 Monotherapy and Anti-PD-1/Anti-CTLA-4 Combined Therapy. Cancer Cell *35*, 238–255.e6. https://doi.org/10.1016/j.ccell.2019.01.003.

34. Riaz, N., Havel, J.J., Makarov, V., Desrichard, A., Urba, W.J., Sims, J.S., Hodi, F.S., Martín-Algarra, S., Mandal, R., Sharfman, W.H., et al. (2017). Tumor and Microenvironment Evolution during Immunotherapy with Nivolumab. Cell *171*, 934–949.e16. https://doi.org/10.1016/j.cell.2017.09.028.

35. Van Allen, E.M., Miao, D., Schilling, B., Shukla, S.A., Blank, C., Zimmer, L., Sucker, A., Hillen, U., Foppen, M.H.G., Goldinger, S.M., et al. (2015). Genomic correlates of response to CTLA-4 blockade in metastatic melanoma. Science *350*, 207–211. https://doi.org/10.1126/science.aad0095.

36. Bhat, P., Leggatt, G., Waterhouse, N., and Frazer, I.H. (2017). Interferon-γ derived from cytotoxic lymphocytes directly enhances their motility and cytotoxicity. Cell Death Dis. *8*, e2836. https://doi.org/10.1038/cddis.2017.67.

37. Intlekofer, A.M., Takemoto, N., Wherry, E.J., Longworth, S.A., Northrup, J.T., Palanivel, V.R., Mullen, A.C., Gasink, C.R., Kaech, S.M., Miller, J.D., et al. (2005). Effector and memory CD8+ T cell fate coupled by T-bet and eomesodermin. Nat. Immunol. *6*, 1236–1244. https://doi.org/10.1038/ni1268.

38. Liu, D., Schilling, B., Liu, D., Sucker, A., Livingstone, E., Jerby-Arnon, L., Zimmer, L., Gutzmer, R., Satzger, I., Loquai, C., et al.

(2019). Integrative molecular and clinical modeling of clinical outcomes to PD1 blockade in patients with metastatic melanoma. Nat. Med. *25*, 1916–1927. https://doi.org/10.1038/s41591-019-0654-5.

39. Cui, C., Xu, C., Yang, W., Chi, Z., Sheng, X., Si, L., Xie, Y., Yu, J., Wang, S., Yu, R., et al. (2021). Ratio of the interferon-γ signature to the immunosuppression signature predicts anti-PD-1 therapy response in melanoma. NPJ Genom. Med. *6*, 7. https://doi.org/10.1038/s41525-021-00169-w.

40. Auslander, N., Zhang, G., Lee, J.S., Frederick, D.T., Miao, B., Moll, T., Tian, T., Wei, Z., Madan, S., Sullivan, R.J., et al. (2018). Robust prediction of response to immune checkpoint blockade therapy in metastatic melanoma. Nat. Med. *24*, 1545–1549. https://doi.org/10.1038/s41591-018-0157-9.

41. Wang, L., Saci, A., Szabo, P.M., Chasalow, S.D., Castillo-Martin, M., Domingo-Domenech, J., Siefker-Radtke, A., Sharma, P., Sfakianos, J.P., Gong, Y., et al. (2018). EMT- and stroma-related gene expression and resistance to PD-1 blockade in urothelial cancer. Nat. Commun. *9*, 3503. https://doi.org/10.1038/s41467-018-05992-x.

42. McDermott, D.F., Huseni, M.A., Atkins, M.B., Motzer, R.J., Rini, B.I., Escudier, B., Fong, L., Joseph, R.W., Pal, S.K., Reeves, J.A., et al. (2018). Clinical activity and molecular correlates of response to atezolizumab alone or in combination with bevacizumab versus sunitinib in renal cell carcinoma. Nat. Med. *24*, 749–757. https://doi.org/10.1038/s41591-018-0053-3.

43. Mariathasan, S., Turley, S.J., Nickles, D., Castiglioni, A., Yuen, K., Wang, Y., Kadel, E.E., III, Koeppen, H., Astarita, J.L., Cubas, R., et al. (2018). TGFβ attenuates tumour response to PD-L1 blockade by contributing to exclusion of T cells. Nature *554*, 544–548. https://doi.org/10.1038/nature25501.

44. Saltz, J. Spatial Organization and Molecular Correlation of Tumor-Infiltrating Lymphocytes Using Deep Learning on Pathology Images. 21.

45. Wu, T.D., Madireddi, S., de Almeida, P.E., Banchereau, R., Chen, Y.-J.J., Chitre, A.S., Chiang, E.Y., Iftikhar, H., O'Gorman, W.E., Au-Yeung, A., et al. (2020). Peripheral T cell expansion predicts tumour infiltration and clinical response. Nature *579*, 274–278. https://doi.org/10.1038/s41586-020-2056-8.

46. Simoni, Y., Becht, E., Fehlings, M., Loh, C.Y., Koo, S.-L., Teng, K.W.W., Yeong, J.P.S., Nahar, R., Zhang, T., Kared, H., et al. (2018). Bystander CD8+ T cells are abundant and phenotypically distinct in human tumour infiltrates. Nature *557*, 575–579. https://doi.org/10.1038/s41586-018-0130-2.

47. Lowery, F.J., Krishna, S., Yossef, R., Parikh, N.B., Chatani, P.D., Zacharakis, N., Parkhurst, M.R., Levin, N., Sindiri, S., Sachs, A., et al. (2022). Molecular signatures of antitumor neoantigen-reactive T cells from metastatic human cancers. Science *375*, 877–884. https://doi.org/10.1126/science.abl5447.

48. Yu, G., Wang, L.-G., Han, Y., and He, Q.-Y. (2012). clusterProfiler: an R Package for Comparing Biological Themes Among Gene Clusters. OMICS A J. Integr. Biol. *16*, 284–287. https://doi.org/10.1089/omi.2011.0118.

49. Mann, H.B., and Whitney, D.R. (1947). On a Test of Whether one of Two Random Variables is Stochastically Larger than the Other. Ann. Math. Statist. *18*, 50–60. https://doi.org/10.1214/aoms/1177730491.

50. Girden, E. (2022). ANOVA. https://doi.org/10.4135/9781412983419.

51. Benesty, J., Chen, J., Huang, Y., and Cohen, I. (2009). Pearson Correlation Coefficient. In Noise Reduction in Speech Processing, I. Cohen, Y. Huang, J. Chen, and J. Benesty, eds. (Springer Berlin Heidelberg), pp. 1–4. https://doi.org/10.1007/978-3-642-00296-0_5.

52. Kim, S. (2015). ppcor: An R Package for a Fast Calculation to Semi-partial Correlation Coefficients. Commun. Stat. Appl. Methods *22*, 665–674. https://doi.org/10.5351/CSAM.2015.22.6.665.

53. Hänzelmann, S., Castelo, R., and Guinney, J. (2013). GSVA: gene set variation analysis for microarray and RNA-Seq data. BMC Bioinf. *14*, 7.

STAR★METHODS

KEY RESOURCES TABLE

REAGENT or RESOURCE	SOURCE	IDENTIFIER
Software and algorithms		
R version 4.3.0	R software foundation	https://www.r-project.org
clusterProfiler 4.8.3	Yu et al.[48]	https://bioconductor.org/packages/release/bioc/html/clusterProfiler.html
ppcor 1.1	Kim et al.[52]	https://cran.r-project.org/web/packages/ppcor/index.html
GSVA 1.48.3	Hänzelmann et al.[53]	https://bioconductor.org/packages/release/bioc/html/GSVA.html
Other		
Gide et al.[33]	EMBL-EBI	ENA: PRJEB23709
Riaz et al.[34]	GEO	GSE91061
Liu et al.[38,16]	dbGaP	phs000452.v3.p1
Cui et al.[39]	China National Center for Bioinformation	HRA000524
Van Allen et al.[35]	dbGaP	phs000452.v2.p1

RESOURCE AVAILABILITY

Lead contact

Further information and requests for resources and reagents should be directed to and will be fulfilled by the lead contact, Eytan Ruppin (eytan.ruppin@nih.gov).

Materials availability

This study did not generate new unique reagents.

Data and code availability

- This paper analyzes existing, publicly available data. These accession numbers for the datasets are listed in the key resources table.
- All original code has been deposited at Github (https://github.com/wbb1813/DETACH.git) and is publicly available as of the date of publication.
- Any additional information required to reanalyze the data reported in this paper is available from the lead contact upon request.

METHOD DETAILS

Transcriptomic data and gene signatures

Gene expression data of TCGA patients were downloaded from GDC: https://portal.gdc.cancer.gov. Transcriptomic data, cell type abundances, and cell-type specific expression profile of ICI treated melanoma cohorts[33,34,38] were retrieved from CODEFACS.[28] The following published gene signatures were obtained from original publications: cytotoxic T lymphocytes (CTL) signature,[4] exhausted T lymphocytes (ETL) signature,[19] reactive T cell signature.[47]

Prediction of ICIs response, patient cohort and clinical end points

We collected five RNA-Seq datasets[33–35,38,39] from melanoma patients undergoing immune checkpoint blockade therapies. These datasets include gene expression profiles of pre-treatment tumors, along with corresponding response information. For each dataset, we normalized expression counts to obtain transcripts per kilobase million (TPM) values. Subsequently, the datasets were divided into subgroups based on the treatment received: PD-1/CTLA-4 monotherapy or a combination therapy involving both PD-1 and CTLA-4 inhibitors.

Response status of ICIs treated melanoma patients based on the RECIST criteria were retrieved from original publications. ''CR/PR'' patients were classified as responders and ''SD/PD'' patients were classified as non-responders. Previously published biomarkers, TIDE,[7] IMPRES,[24] CD274 (PDL1),[13] stroma EMT,[41] CD8 T cell effector,[42] and TGFB,[43] were collected from the literature and tested for association with response to ICIs therapy. Sample-wise scores were calculated from bulk RNA-seq data using TPM values and following the methodology described in corresponding studies. Genes with unavailable expression data were excluded from calculations of gene signature scores. The predictive utility of these immune signatures was evaluated with AUC values derived from ROC curves of gene signature scores and odd ratio calculated from confusion matrix. Cutoffs for determining responders and non-responders were optimized by maximizing the sum of specificity and sensitivity.

DETACH

To identify genes that can mitigate the correlation between CTL and ETL activities, DETACH employed a variable interaction test in a multivariate linear regression to TCGA SKCM cohort.

For each gene G, we performed the following regression:

$$Cytotoxicity = \beta_0 + \beta_1 * Exhaustion + \beta_2 * G + \beta_3 * Exhaustion * G$$

Where $Cytotoxicity$ and $Exhaustion$ denote the CTL and ETL activity levels which were estimated by calculating the enrichment score for CTL and ETL signatures. G represents the expression level of gene G in a tumor.

To further understand the variable interaction test, we can rewrite the model as follows:

$$Cytotoxicity = (\beta_1 + \beta_3 * G) * Exhaustion + \beta_2 * G + \beta_0$$

The association between CTL and ETL activities is $(\beta_1 + \beta_3 * G)$. The coefficient β_1 is typically positive because the CTL and ETL activities are positively correlated (Figure 1A). The expression value used in this model are positive values, which means a negative coefficient β_3 will reduce the positive association between CTL and ETL activities, whereas a positive coefficient will enhance the positive association. The DETACH signature was identified according to the t value: β_3 / $StdErr(\beta_3)$ and FDR. A total of 66 genes had significant negative coefficient values and were identified as *DETACH signature* using cutoff T value < 0 and FDR <= 0.01.

Determination of thresholds for patients with high DS score

A series of thresholds, ranging from 5% to 100% in increments of 5%, were applied to subset melanoma patients from TCGA SKCM, Gide et al., Riaz et al., Van Allen et al., Cui et al., and Liu et al. cohorts. Pearson correlation was used to calculate the CTL and ETL correlation for each subgroup. Individual thresholds for each cohort were determined by identifying the percentage at which the CTL and ETL exhibited the lowest correlation coefficient value. It is worth noting that the thresholds were set to be greater than 10% to ensure an adequate inclusion of samples. Specifically, the individual thresholds for TCGA SKCM, Gide et al., Riaz et al., Van Allen et al., Cui et al., and Liu et al. cohorts were found to be 25%, 15%, 15%, 15%, 15%, and 15%, respectively.

Robustness evaluation of DETACH signature

The TCGA SKCM dataset was down sampled to 90%, 80%, and 70% a hundred times at each percentage to generate pseudo-new datasets. Subsequently, DETACH was applied to these downsampled datasets as well as three independent ICB datasets[33–35] to evaluate the ability of each gene to decouple ETL and CTL activity. The enrichment score of the DETACH signature and a control gene set, randomly selected to match the number of genes in the DETACH signature, against the down sampled and three independent ICB datasets, was assessed using GSEA. A high positive Normalized Enrichment Score (NES) indicates that genes in the gene set are ranked at the top of the gene list identified using the down sampled and independent ICB datasets. Statistical significance of the NES between the DETACH and control gene sets was calculated using a one-tailed Wilcoxon test.

TCGA Tumor Infiltrated Lymphocyte (TIL) patterns

Tumor Infiltrated Lymphocyte (TIL) patterns for TCGA SKCM patients were retrieved from a study.[44] Briefly, pathology sides were used to characterize the TILs patterns for TCGA patients. TILs patterns were visually assigned by a pathologist into one of five categories:

1. Brisk, diffuse: diffused TILs scattered throughout at least 30% of the area of the tumor.
2. Brisk, band-like: band-like boundaries formed by TILs bordering the tumor at its periphery.
3. Non- brisk, multi-focal: loosely scattered TILs present in less than 30% but more than 5% of the area of the tumor.
4. Non-brisk, focal: loosely scattered TILs present less than 5% but greater than 1% of the area of the tumor.
5. None: few TILs were present involving 1% or less of the area of the tumor.

Gene function enrichment analysis

Gene set enrichment analysis of DETACH signature genes was conducted against the GO BP database using clusterProfiler[48] with the follow settings: OrgDb = org.Hs.eg.db, ont = "MF", pAdjustMethod = "BH", pvalueCutoff = 0.01.

QUANTIFICATION AND STATISTICAL ANALYSIS

Differences between two-continuous variable were assessed using Wilcoxon rank sum test.[49] ANOVA test[50] was used to determine if there is a statistically significant difference between more than two categorical groups. Association between two-continuous variable were measured by Pearson correlation.[51] R package "ppcor"[52] was used to eliminate the effect of other variables when assessing the correlation between CTL and ETL activities.[52] Significance levels were denoted using asterisks (* P<0.05, ** P<0.01, *** P<0.001, **** P<0.0001), with 'ns' indicating non-significance (P>=0.05).